

Developmental expression of calretinin in the mouse cochlea

Wenjing Liu,¹ Yongchun Zhang,² Cheng Liang,² Xuefan Jiang¹

¹Otolaryngology & Head and Neck Center, Cancer Center, Department of Otolaryngology, Zhejiang Provincial People's Hospital (Affiliated People's Hospital, Hangzhou Medical College), Hangzhou

²Department of Otorhinolaryngology-Head and Neck Surgery, Zhongda Hospital, Southeast University, Nanjing, China

ABSTRACT

This study investigated the expression of calretinin (CR) in the mouse cochlea from embryonic day 17 (E17) to adulthood through immunofluorescence. At E17, CR immunoreactivity was only detected in the inner hair cells (IHCs). At E19, the IHCs and spiral ganglion neurons (SGNs) begin to express CR. At birth, CR immunoreactivity was confined primarily to the IHCs and the majority of the SGNs, as identified by TUJ1, both the cytoplasm and the nucleus of SGNs exhibited CR positivity. At postnatal day 2 (P2), auditory nerve fibers reaching the IHCs were stained for CR. CR continued to be expressed in the IHCs, whereas only single row of outer hair cells (OHCs) were positive for CR. By P5, CR expression was evident in IHCs and the three rows of OHCs, with SGNs soma and their neurite projections also displaying CR immunoreactivity. From P8 through adulthood, CR expression persisted in the SGNs and their afferent neurite projections to the IHCs, as well as in IHCs and OHCs. Dual labeling of CR with afferent nerve marker neurofilament 200 (NF200) demonstrated that NF 200-positive SGN somas were encompassed by CR-labeled plasma membrane of SGNs, and NF 200 was co-localized with CR in the afferent nerve fibers innervating the IHCs. We also described the expression of peripherin, a marker for type II SGNs, in the mouse cochlea at various postnatal stages. Peripherin showed a distinct spatio-temporal expression compared to CR in auditory nerve fibers. No co-expression of peripherin and CR was detected in adult. Dynamic expression patterns of CR in the embryonic and postnatal cochlea supported its roles in cochlear development.

Key words: calretinin; cochlea; mouse; immunofluorescence.

Correspondence: Xuefan Jiang, Otolaryngology & Head and Neck Center, Cancer Center, Department of Otolaryngology, Zhejiang Provincial People's Hospital (Affiliated People's Hospital, Hangzhou Medical College), Hangzhou, China. E-mail: jiangxuefan1@163.com

Contributions: WL, performed the experiments, conceived the study and wrote the manuscript; YZ, CL, XJ, helped to edit and revise the manuscript. All the authors read and approved the final version of the manuscript and agreed to be accountable for all aspects of the work.

Conflict of interest: the authors declared no potential conflicts of interest with respect to the research, authorship, and/or publication of this article.

Ethics approval: all animal studies, including the mice euthanasia procedure, were approved by the Animal Care and Use Committee of the Southeast University, Nanjing, China (approval no. 20200402025).

Funding: this work was supported by the National Natural Science Foundation of China (no. 82000987) and the Natural Science Foundation of Jiangsu Province (no. BK20200394).

Acknowledgments: we thank Dr. Chuang Li (Washington University in St. Louis) for the English language review.

Introduction

Calretinin (CR), parvalbumin, and calbindin are the three most abundant and extensively studied calcium-binding buffer proteins in the nervous system.¹ Their widespread presence has been reported in the mammalian cochlea, indicating indispensable roles in auditory function.^{2,3} CR, a 29 kilodalton protein, belongs to the EF-hand family of calcium-binding proteins and is crucial for maintaining intracellular calcium homeostasis.⁴ CR is widely expressed across normal and pathological human tissues, serving as an immunohistochemical marker in diagnostic pathology, particularly for human benign and malignant mesothelial cells.^{5,6} Calbindin-D28K (CaBP28K) shares homology with CR, with 58% identical residues.⁷ Previous studies have shown specific expression of CaBP28K in the greater epithelial ridge of the immature mouse cochlea,⁸ while the immunolocalization of CR was associated with cochlear afferent fibers, suggesting distinct physiological functions.⁹ CR expression was observed in various auditory neurons, including those in the cochlear nuclei and superior olivary complex located in the brainstem, where its expression at neonatal stages was associated with early development of the auditory brainstem.¹⁰ Increased CR immunostaining in the cochlear nuclei and spiral ganglion neurons (SGNs) was linked to protection against noise-induced hearing loss.¹¹ Furthermore, its function was related to the afferent innervation of the inner hair cells (IHCs) by type I SGNs.^{12,13} Genetic disruption of CR could affect exocytosis and sound encoding at the synapses of mouse IHCs and SGNs.¹⁴ However, its exact physiological role in the cochlea remains complex and hypothetical. Understanding the unique distribution of each calcium-binding proteins could shed light on their roles in cochlear function and better understanding of how calcium levels are controlled within the cochlea.¹⁵ The detailed analysis of temporal and spatial expression of CR in the central nervous system was proposed to be essential in the field of brain development research.¹⁶ The expression of CR in the developing and mature mammalian cochlea was not exhaustively described, as previous studies provided some information regarding CR immunoreactivity during cochlear development,¹⁷⁻¹⁹ but specific hair cell markers for CR have not been reported to be localized in the outer hair cells (OHCs) prior to the hearing onset and in adult. Also, conflicting findings were reported in the literature (for example, CR expression was detected in the IHCs, supporting cells and the spiral limbus in the guinea pig cochlea^{20,21}), possibly due to methodological limitations or differences in immunochemical staining techniques and species difference.

In the present study, we investigated in detail the expression pattern of CR in the developing and mature mouse cochlea: our findings revealed early and stable expression of CR in the SGNs and their afferent neurite projections to the IHCs, further emphasizing its roles in the auditory afferent neurotransmission.²² The developmentally-regulated expression of CR in the mouse cochlea underscored its significance in cochlear ontogeny. Additionally, we described the developmental expression of peripherin, a marker for type II SGNs and type II afferent fibers,^{23,24} in the postnatal and adult mouse cochlea. CR and peripherin exhibited different patterns of expression, further substantiating that CR marks type I afferent fibers.

Materials and Methods

Animals

All animal studies, including the mice euthanasia procedure,

were conducted in compliance with the regulations and guidelines of Southeast University institutional animal care, adhering to the standards set by the Association for Assessment and Accreditation of Laboratory Animal Care (AAALAC) and the Institutional Animal Care and Use Committee (IACUC) guidelines.

Western blotting

Western blotting was conducted using extracts from samples of the entire cochlea of mice aged from postnatal day 0 (P0), P5, P8, P14 to P28. Cochlear tissues were homogenized in ice-cold RIPA Lysis Buffer (50 mM Tris-HCl, pH 7.6, 150 mM NaCl, 1% SDS, 1% Triton X-100, and 0.1 mM EGTA). The cochlear lysates were then separated *via* SDS-PAGE and transferred electrophoretically onto nitrocellulose membranes. Subsequently, the membranes were blocked with non-fat milk, followed by immunoblotting using rabbit anti-CR antibodies (dilution 1:200, #92635S, Cell Signaling Technology, USA). A rabbit anti-GAPDH antibody (1:1000; #KGAA002; Kagi biotech, Nanjing, China) served as an internal loading control. The protein bands were visualized using horseradish peroxidase-conjugated secondary antibody and were detected with a chemiluminescence reagent (Biyuntian). The levels of target proteins were quantified by the Quantity One System (Bio-Rad, Hercules, CA, USA).

Immunofluorescence

Intraperitoneal injection of 10% chloral hydrate (0.2 mL/100 g) was used to anesthetize pregnant (gestational days 17-19) and postnatal (P0-P28) BALB/c mice. Embryos were harvested at embryonic days (E) 17 and 19, Embryos were quickly decapitated, and their cochleae were dissected in ice-cold 4% paraformaldehyde in 0.1 M phosphate buffer (pH 7.4). Postnatal mice were intracardially perfused with saline followed by 4% paraformaldehyde in 0.1 M phosphate buffer (pH 7.4). The detailed methods and procedures of immunofluorescence staining were described in our previous study.^{8,25} Briefly, after perilymphatic perfusion with the fixative mentioned above, cochlea was postfixed in the same solution for 35 min at room temperature. The cochlea from mice older than P5 was decalcified in 10% EDTA at pH 7.4. Following decalcification, the cochleae were immersed in a sucrose gradient (15% for 3 h and 30% overnight). Subsequently, cochlear tissues were embedded in an optimum cutting temperature compound at 4°C for 2.5 h, rapidly frozen at -20°C, and cryoembedded specimens were then sectioned into serial sections (8 µm) on a cryostat, mounted on glass slides.

Cochlear cryosections were treated for 45 min with 10% donkey serum and 0.3% Triton X-100 in PBS at room temperature to enhance cell membranes permeability to antibodies. The sections were then incubated with primary antibodies diluted in 0.01M PBS overnight or longer at 4°C. Primary antibodies used were as follows: rabbit anti-CR antibodies (dilution 1:200, #92635S; Cell Signaling Technology, Danvers, MA, USA), mouse anti-CR antibodies (1:100, #MAB1568; Merk Millipore, Burlington, MA, USA), mouse anti-synaptophysin antibodies (1:200, #9020, Cell Signaling Technology), Sox2 monoclonal antibody (Btjce), Alexa Fluor™ 488 (1:100, #53-9811-82; Invitrogen, Waltham, MA, USA), mouse anti-TUJ1 antibody (1:200; BioLegend, San Diego, CA, USA), mouse anti-neurofilament 200 antibodies (1:200; Boster Bio, Pleasanton, CA, USA), rabbit anti-peripherin antibodies (1:50, ab246502; Abcam, Waltham, MA, USA), In co-staining experiments, CoraLite 594-conjugated phalloidin (1:250, #PF00003; Proteintech, Wuhan, China) was applied to detect F-actin of the hair cells of the organ of Corti. After rinsing three times for 15 min in the 0.01 M PBS, the slides were incubated for 1 h at 37°C with the following secondary antibodies: donkey anti-rabbit IgG conjugated with Alexa 488 or 555 (1:250; Yeasen, Shanghai,

China), donkey anti-mouse IgG conjugated with Alexa 555 or 597 (1:400; Beyotime, Haimen, China). The control sections were incubated with 0.01 M PBS, in the absence of primary antibodies. In addition, rabbit (DA1E) monoclonal antibody IgG XP Isotype control (#3900; Cell Signaling Technology) was used as a negative control, instead of CR antibody. Then, the sections were washed with PBS, fluorescence was preserved by sealing specimens with an antifade mounting medium containing 4',6-diamidino-2-phenylindole (Biyuntian Biotechnology Co., Ltd., Shanghai, China). Cryostat sections were examined using a Zeiss (LSM900) laser scanning confocal microscope with 10× [numerical aperture (NA) = 0.45], 20× (NA = 0.8), 40× (NA = 0.95) and 63× oil (NA = 1.4) objectives at 1024 × 1024 pixels. Zen3.0 acquisition software was used. Immunostaining presented in figures was representative of three individual experiments. Images were cropped and resized using Adobe Photoshop CC 2019.

Results

Expression patterns of CR in the mouse cochlea during the late embryonic stages of development by immunofluorescence

Western blotting analysis confirmed the specificity of the polyclonal anti-CR antibody employed in this study. A prominent band with a molecular weight of approximately 29kDa, corresponding to CR protein, was detected in the entire mouse cochlea across various developmental stages, validating the antibody's suitability for immunohistochemistry (Figure 1).

In this investigation, CR expression in the mouse cochlea at different developmental stages was explored. Consistent with the Dechesne *et al.*¹⁸ CR immunoreactivity was detectable at later

embryonic stages. Additionally, during early postnatal developmental stages, gradients in CR staining between cochlear turns were observed. Consequently, our study focused on the expression pattern of CR in the middle turn of the postnatal mouse cochlea. Here, age-dependent changes in CR distribution were demonstrated. Prior to birth, at E17 (the earliest stage studied), double-immunofluorescence analysis with the supporting cell marker Sox2 showed only IHCs cytoplasm in the organ of Corti in the

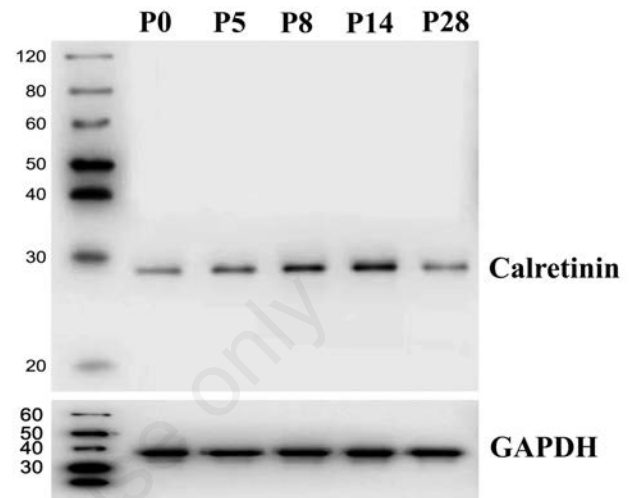


Figure 1. Western blotting validation of the anti-CR monoclonal antibody. A strong band at approximately 29 kDa is detected in mouse cochlea at P0, P5, P8, P14 and P28. GAPDH serves as the loading control for Western blot.

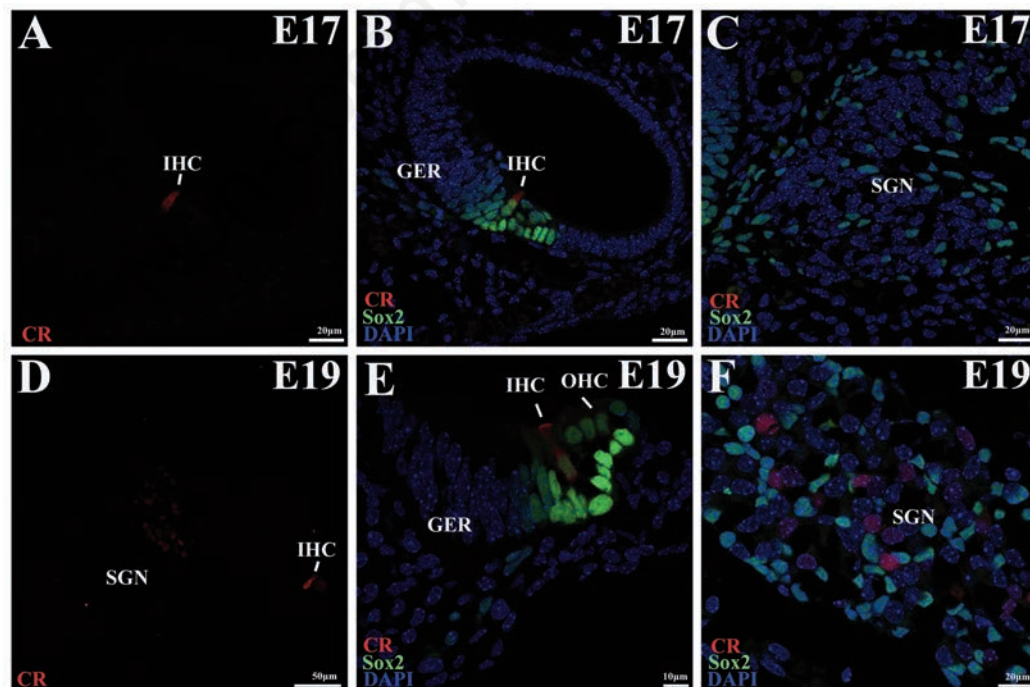


Figure 2. CR immunolabeling in the mouse cochlea at E17 and E19. **A-C)** At E17, CR immunolabeling was only found in the IHCs in the middle turn. Sox2 labeled HCs and supporting cell nuclei in the organ of Corti, as well as the glial cells. **D-F)** At E19, CR immunoreactivity was observed in the IHCs, and its expression occurred in the SGNs, Sox2-positive glial cells were negative for CR. GER, greater epithelial ridge; IHC, inner hair cell; OHC, outer hair cell; SGN, spiral ganglion neuron.

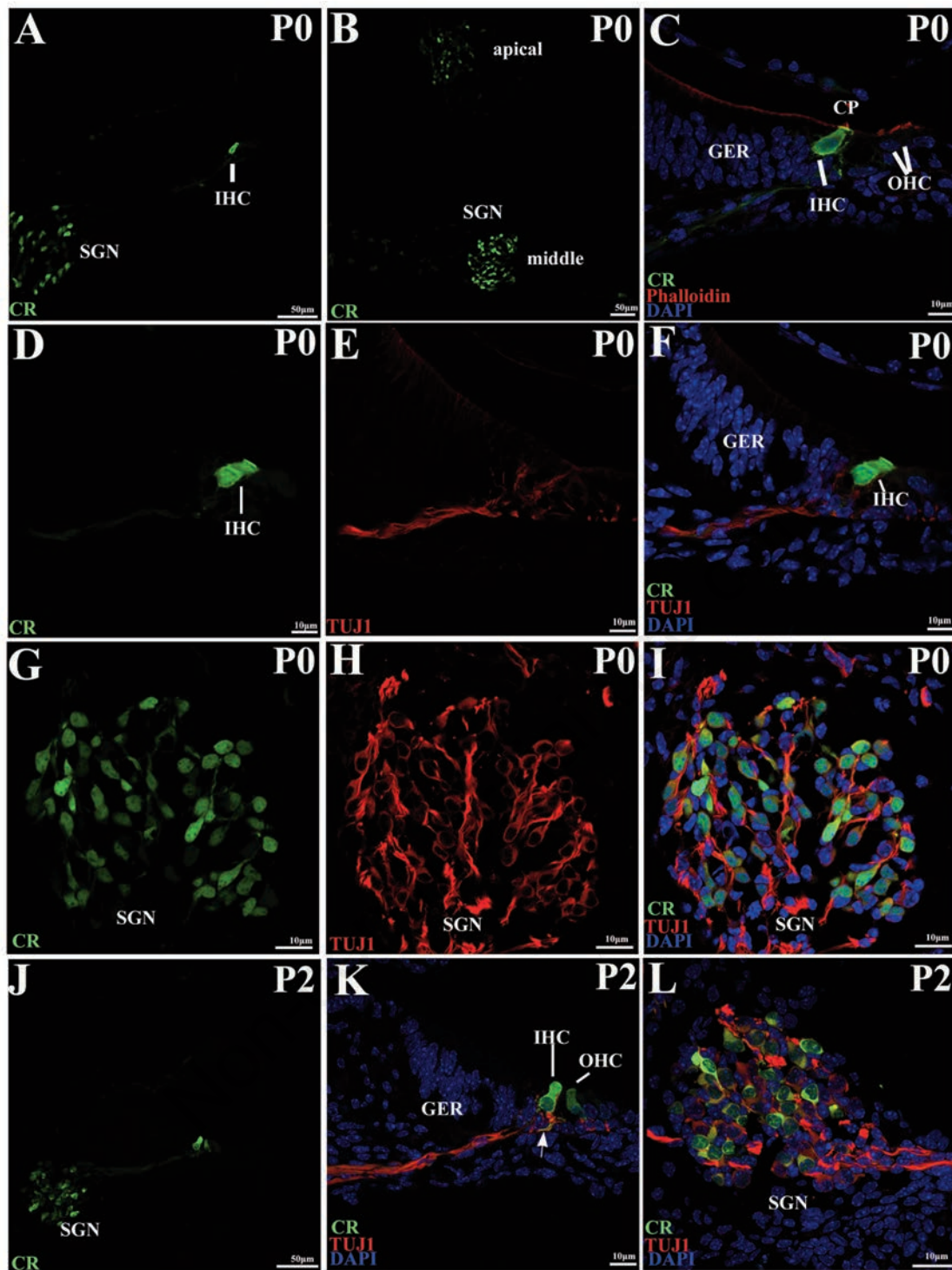


Figure 3. CR immunolabeling in the mouse cochlea at P0 and P2. **A,B)** A low-magnification view of the cross-sections of the mouse cochlea labeled with CR (green) at P0; in the apical turns, CR was not expressed in the IHCs, but only in the SGNs; in the middle turns, both IHCs and most of SGNs were immunoreactive for CR. **C)** Detail of CR (green) and phalloidin (red) labeling in the middle turn of P0 mouse cochlea; CR was not detectable in the greater epithelial ridge; CR immunoreactivity was only present in the IHC, colocalization of CR with phalloidin was found in the cuticular plates of IHCs. **D-F)** Double labeling with CR (green) and neural marker TUJ1 (red) expression in the peripheral processes of P0 cochlea and the merged image + DAPI; CR immunoreactivity was virtually absent under the IHCs. **G-I)** Double labeling of CR (green) with SGNs marker TUJ1 (red) expression in the P0 SGNs and the merged image + DAPI; CR immunolabeling was present in both the cytoplasm and the nucleus of SGNs identified by TUJ1. **J)** Overview of CR immunolabeling in the mouse cochlea at P2. **K)** Double labeling of CR (green) with TUJ1 (red) expression in the P2 SGNs and the merged image + DAPI; CR was detectable in the OHCs, but not three rows of OHCs. CR immunolabeling was also observed in the peripheral processes (arrowheads) reaching the IHCs. **L)** Double labeling of CR (green) with TUJ1 (red) expression in the P2 SGNs and the merged image + DAPI; a small population of SGNs was unstained for CR. GER, greater epithelial ridge; IHC, inner hair cell; OHC, outer hair cell; SGN, spiral ganglion neuron; CP, cuticular plates.

middle turn exhibited CR immunoreactivity,⁸ no CR labeling was detected in the apical turn. Sox2-positive HCs and supporting cell nuclei were also not labelled by CR (Figure 2 A-C). At E19, CR maintains its expression in the IHCs, but no OHCs labeling was detected. CR immunolabelling was observed in the SGNs in the middle turn (Figure 2D-F).

Expression patterns of CR in the mouse cochlea during postnatal development by immunofluorescence

At birth, CR maintains its expression in the IHCs in the organ of Corti and SGNs, while no CR positivity is observed in the IHCs in the apical turn, and other structures in the organ of Corti showed no immunoreactivity for CR (Figure 3 A-C). TUJ1-labeled periph-

eral neurites of the SGNs appeared almost negative for CR at this stage (Figure 3D-F). However, most SGNs identified by the TUJ1 immunostaining, but not all, were immunoreactive for CR, present in both the cytoplasm and the nucleus of the SGNs (Figure 3 G-I). At P2, CR began to be expressed in the OHC and the peripheral neurites of the SGNs innervating the IHCs (Figure 3 J-L). By P5, three rows of OHCs and IHCs displayed CR immunoreactivity, CR and phalloidin were colocalized in the cuticular plates (Figure 4 A-C). Besides SGNs, CR staining was also evident in their afferent neurite projections to the base of the developing IHCs (Figure 4 D-I). At P8, nerve fibers in the cochlear modiolus were CR positive. CR was expressed in the IHCs and SGN in all three cochlear turns (Figure 5A). At this stage, CR expression was detected in the numerous round-shaped plasma membrane of SGNs, rather than

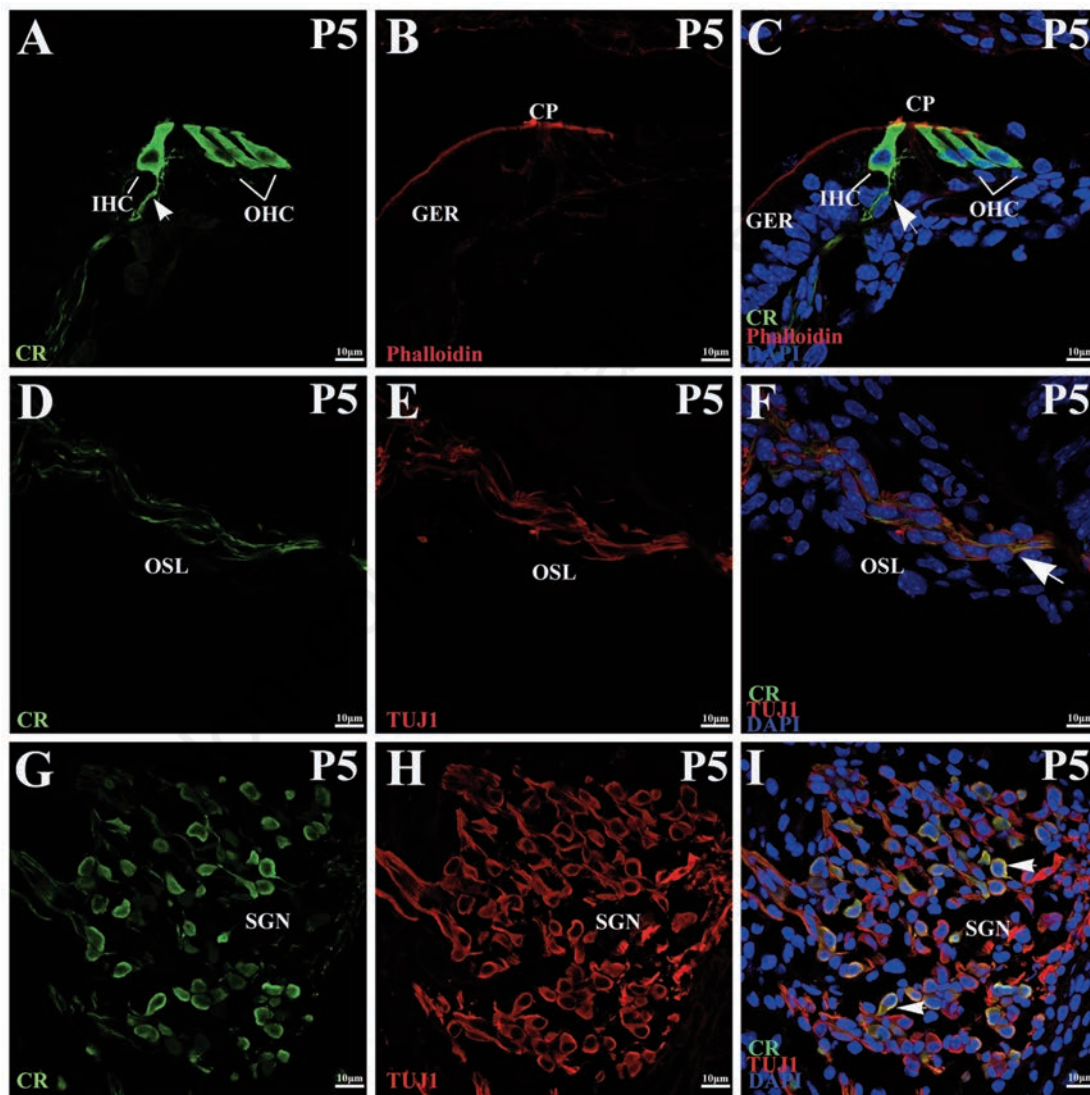


Figure 4. CR immunolabeling in the mouse cochlea at P5. **A-C)** Detail of CR (green) and phalloidin (red) labeling in the middle turn of P5 mouse cochlea; CR was detectable in the IHC and OHC, colocalization of CR with phalloidin was found in the cuticular plates of the IHC and OHC; CR-positive cochlear neural fibres (arrowheads) reached the IHCs. **D-F)** Double labeling with CR (green) and neural marker TUJ1 (red) expression in the peripheral processes of P5 cochlea and the merged image + DAPI; CR partly colocalized with TUJ1 in the peripheral processes (arrowheads) in the P5 osseous spiral lamina. **G-I)** Double labeling with CR (green) and SGNs marker TUJ1 (red) expression in the P5 SGNs and the merged image + DAPI; most of CR-expressing SGNs somas (arrowheads) were double-labeled by TUJ1. GER, greater epithelial ridge; IHC, inner hair cell; OHC, outer hair cell; SGN, spiral ganglion neuron; CP, cuticular plates; OS, osseous spiral lamina.

long process on the same side of the SGNs bodies (Figure 5B). CR-positive distal peripheral nerve processes of the SGNs formed contacts with the IHC base. Previous fluorescent histochemical studies suggested that CR-labelled nerve fibres in the mammalian cochlea represented afferent fibres and correlated with the type I SGNs neurite innervation pattern.^{26,27} To further demonstrate CR-positive neural elements, we utilized the dual-labeling of CR with the presynaptic protein synaptophysin and neurofilament 200 (NF 200).^{28,29} NF 200 identified SGNs and afferent nerve fibers. CR-positive afferent nerve fibers did not colocalize with synaptophysin-positive presynaptic nerve endings beneath the IHCs, indi-

cating their non-efferent nature (Figure 5C). CR-positive nerve terminals predominantly innervated the pillar sides of IHCs and colocalized with NF 200 (Figure 5D-F). CR staining was evident in the peripheral neurites within the osseous spiral lamina, showing double-labeling with NF 200 (Figure 5G-I). At the onset of hearing, CR expression persisted in the IHCs, OHCs, and nerve fibers innervating the IHCs (Figure 6 A-C). Portions of NF 200-positive nerve fibers lacked CR immunoreactivity within the osseous spiral lamina at P14 (Figure 6 D-F). CR continued to be present in the plasma membrane of SGNs (Figure 6 G-I). In the adult cochlea, CR displayed a similar expression pattern as at P14, with afferent

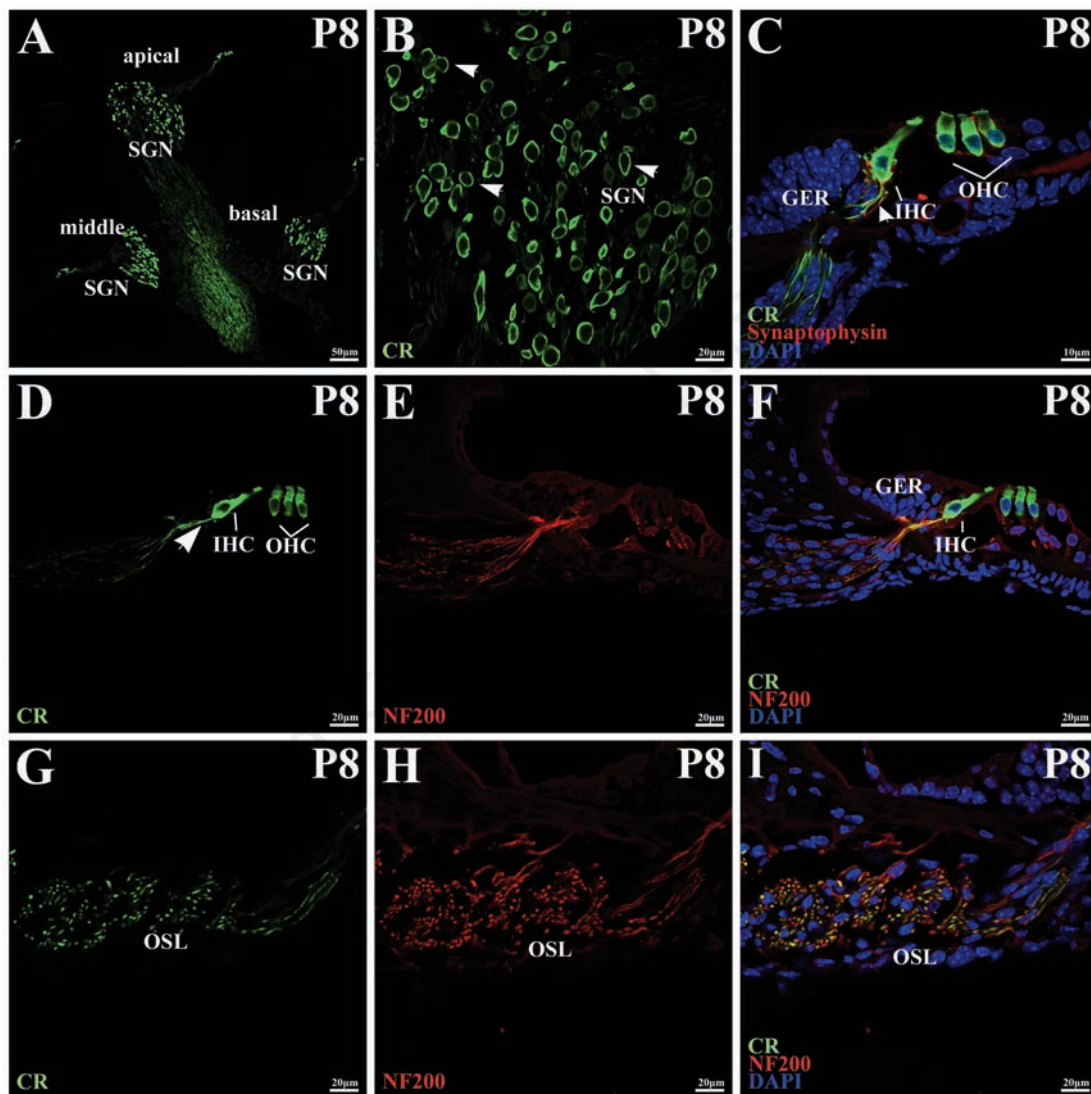


Figure 5. CR immunolabeling in the mouse cochlea at P8. **A,B**) A low-magnification view of the cross-sections of the mouse cochlea labeled with CR (green) at P8; the expression of CR in the IHCs and OHCs was observed in the apical turns; nerve fibers within the cochlear modiolus were immunoreactive for CR; many CR-positive SGNs (arrowheads) were membranous and round-shaped. **C**) Dual-labeling of CR (green) with efferent terminals marker synaptophysin (red) in the P8 organ of Corti; presynaptic synaptophysin spots underneath the IHCs did not coexpressed with CR-labelled afferent nerve fibers, CR-labelled afferent terminals (arrowheads) was seen in contact with the IHCs. **D-F**) Dual-labeling of CR (green) with afferent terminals marker NF200 (red) in the P8 organ of Corti; CR-labelled nerve fibres (arrowheads) innervating the pillar side of the IHC were coexpressed with NF200. **G-I**) Double labeling with CR (green) and NF200 (red) in the P8 osseous spiral lamina and the merged image + DAPI; CR was colocalized with NF200 in the P8 osseous spiral lamina. GER, greater epithelial ridge; IHC, inner hair cell; OHC, outer hair cell; SGN, spiral ganglion neuron; CM, cochlear modiolus; CP, cuticular plates; OSL, osseous spiral lamina.

synaptic terminals under the IHCs and peripheral afferent processes maintaining CR expression and co-localizing with NF 200 (Figure 7 A-F). CR immunolabelling in the adult SGNs also showed membranous localization (Figure 7 G-I). Co-staining of CR and type II SGNs marker for peripherin revealed no co-localization of CR with peripherin-positive type II SGNs (Figure 7 J-L). Considering the preferential expression of CR in type I SGNs and the significant morphological and functional differences between type I and type II SGNs, we also examined the immunolocalization of the type II SGN marker peripherin in the developing mouse cochlea. Peripherin immunoreactivity was virtually absent prior to

birth (*data not shown*), inconsistent with previous studies.^{23,24} However, from P1 through adulthood, our immunolabeling data on the distribution pattern of peripherin in the mouse cochlea was largely consistent with previous results. At P1, peripherin-positive type II afferent nerve fibers were observed under the IHCs and OHCs (Figure 8A), however, minimal peripherin immunolabeling was detected in the SGNs (Figure 8 B,C). By P5, type II SGNs began to express peripherin, which was confined to type II afferent nerve fibers under the OHCs (Figure 8 D-F). At P8, peripherin-positive type II SGN neurites extended beyond the floor of the tunnel of Corti to the OHCs, with a small subset of type II SGNs

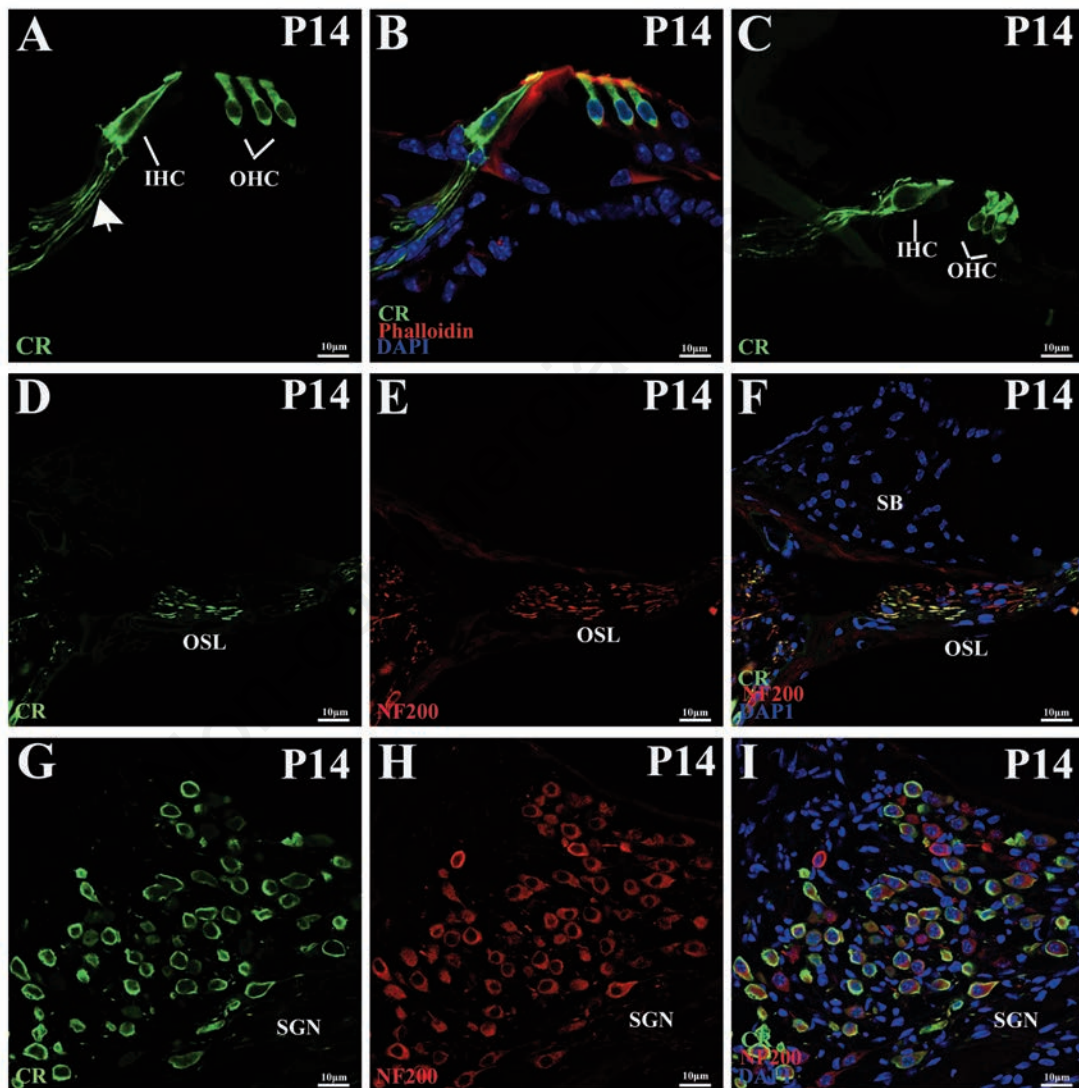


Figure 6. **A,B**) Detail of CR (green) and phalloidin (red) labeling in the middle turn of P14 mouse cochlea; CR was detectable in the P14 IHC and OHC, colocalization of CR with phalloidin was found in the cuticular plates of the hair cells; CR-positive cochlear neural fibres (arrows) preferentially contacted the pillar side of the IHC. **C**) CR immunolabeling in the peripheral neurites innervating the IHC was also observed in the basal turn of P14. **D-F**) Double labeling with CR (green) and NF200 (red) in the P14 osseous spiral lamina and the merged image + DAPI; CR was colocalized with NF200 in the P14 osseous spiral lamina. **G-I**) Double labeling with CR (green) and NF200 (red) expression in the P14 SGNs and the merged image + DAPI; CR immunolabeling was present in the plasma membrane of SGNs; NF200-positive the cytoplasm of SGNs appeared surrounded by CR-positive the plasma membrane of SGNs. IHC, inner hair cell; OHC, outer hair cell; SGN, spiral ganglion neuron; OSL, osseous spiral lamina; SB, spiral limbus.

immunoreactive for peripherin (Figure 8 G,H). At this developmental stage, no co-localization of peripherin with the neuronal marker TUJ1 was observed (Figure 8I). At P14, there was an absence of CR immunoreactivity in the type II afferent fibers (*not shown*). Co-staining of peripherin and NF200 revealed co-localization of peripherin-positive type II SGNs with NF200 (Figure 8 J-L), as previously shown.

Discussion

In this study, we describe in detail the spatio-temporal expression of CR in the mouse cochlea ranging from E17 to P28. Using double immunofluorescence staining for CR with either peripherin

or synaptophysin, our results showed that CR was specifically localized to type I SGN and their afferent neurite projections to IHCs, supporting further a role of CR in the formation of afferent neurotransmission in the mouse cochlea. It is well established that primary auditory nerve fibers show a spontaneous activity prior to the onset of hearing, which play an important role in synaptic maturation and refinement of auditory circuits.³⁰ Cochlea ectomy studies showed that cochlea removal at P5 lead to a decreased CR immunostaining in terminals originating from auditory nerve fibers, which were probably caused by a loss of spontaneous activity.³¹ CR is known to be required for normal developmental process of both the central and peripheral nervous systems, including axon guidance and synaptogenesis.³²⁻³⁴ Prior studies of cochlear development in mice have showed that the early postnatal period, until the onset of hearing generally around P12-P14, is crit-

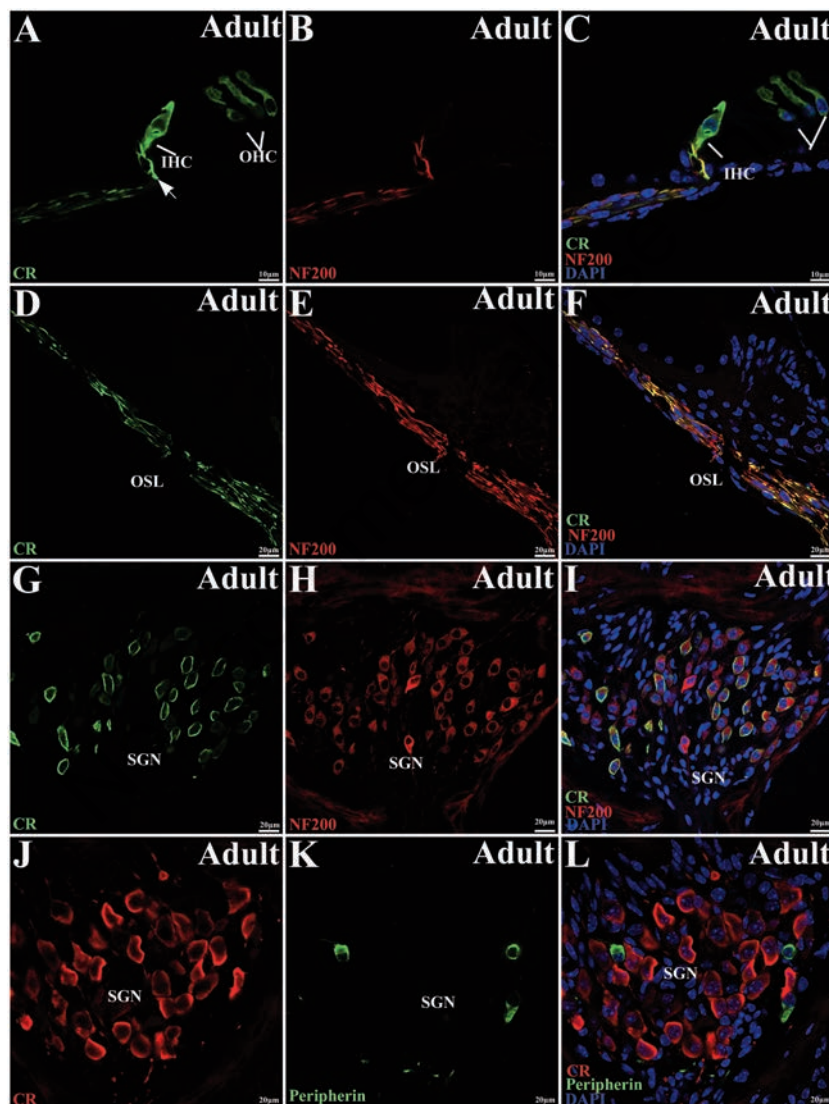


Figure 7. **A-C)** Detail of CR (green) and NF200 (red) labeling in the middle turn of adult mouse cochlea; afferent terminals (arrows) innervating the IHCs are double positive for CR (green) and NF200 (red). **D-F)** Double labeling with CR (green) and NF200 (red) in the adult osseous spiral lamina and the merged image + DAPI. CR was colocalized with NF200 in the adult osseous spiral lamina. **G-I)** Double labeling with CR (green) and NF200 (red) expression in the adult SGNs and the merged image + DAPI; CR immunolabeling was present in the plasma membrane of adult SGNs. CR-positive the plasma membrane of SGNs was not colocalized with NF200-positive the cytoplasm of SGNs. **J-L)** Double labeling with CR (red) and peripherin (green) in the adult SGNs and the merged image + DAPI; CR was not colocalized with peripherin in the adult SGNs. IHC, inner hair cell; OHC, outer hair cell; SGN, spiral ganglion neuron; OSL, osseous spiral lamina.

ical for the correct establishment of afferent innervation to the cochlear sensory hair cells, with significant pruning and refinement of SGN neurites.^{35,36} To the best of our knowledge, this study is the first to demonstrate the differential expression of CR in the afferent neurite projections to the developing IHCs during this critical period. Between P2 and P5, when the IHC innervation is exclusively from type I SGNs, CR-labeled SGN peripheral processes extended into the bases of IHCs. As the cochlear afferent innervation reorganized towards an adult-like state, CR maintained its expression in the SGNs and their distal neurite processes innervating the IHC, indicating that CR expression in the cochlea may play important roles in afferent synaptic pruning and maturation. CR expression in the SGNs and cochlear afferent nerve fibers has been reported to play a role in neuroprotection against diabetic neuropathy.³⁷ Additionally, CR's neuroprotective role against age-

related calcium overload in the auditory neurons has been established.^{38,39} The expression of CR coincides well with neuronal differentiation and neurogenesis,^{40,41} and knock down of CR can lead to disrupted development of motor neurons.⁴² Apart from its participation in the development of cochlear neural circuitry, expression of CR in sensory hair cells was developmentally regulated. CR expression was shown in the differentiating IHCs as early as E17, and the expression of CR in the IHCs was earlier than that in the OHCs. This result is consistent with the idea that the IHCs mature before the OHCs.⁴³ As the maturation of the mouse cochlea proceeded, the expression of CR in the IHCs and OHCs was maintained throughout adulthood, suggesting its expression was associated with the differentiation and maturation of sensory hair cells, where CR may be relevant to increased Ca^{2+} buffering capacity.⁴⁴ Co-staining of CR and phalloidin showed its specific expression in

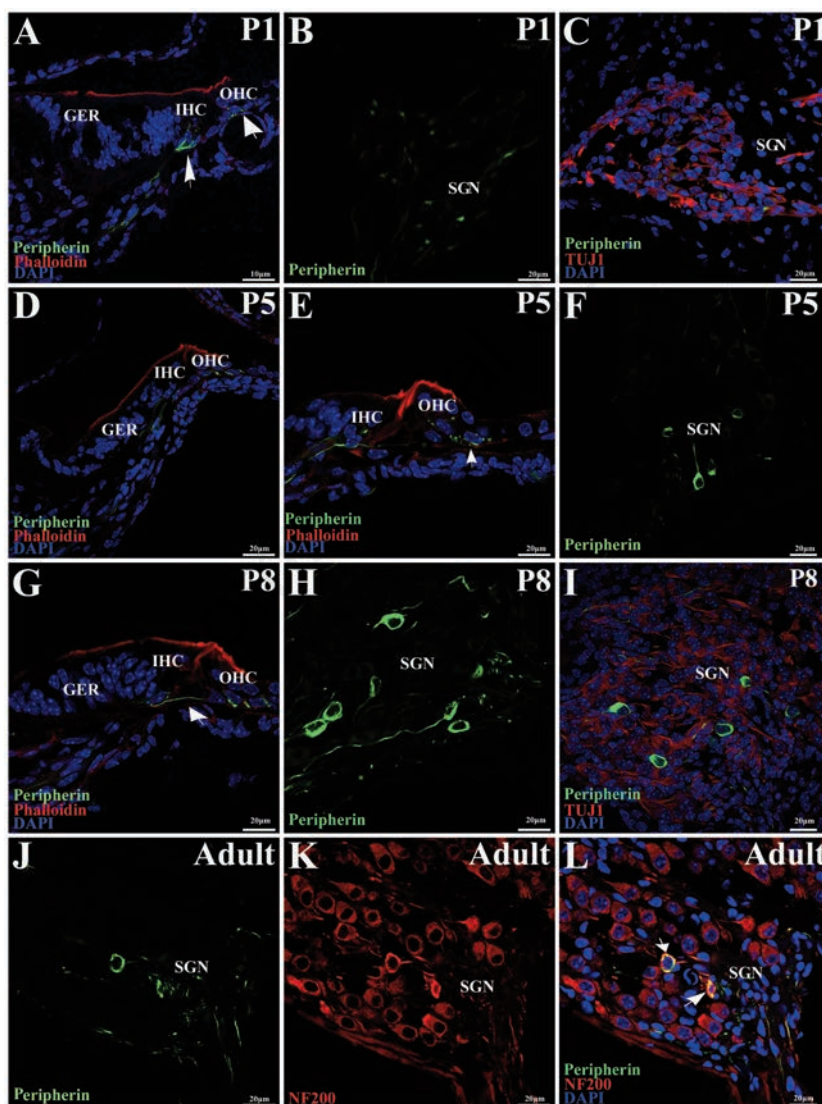


Figure 8. A) Detail of peripherin (green) immunolabeling in the P1 mouse cochlea; peripherin-positive type II cochlear afferent nerve fibers were found below the IHCs and OHC. B,C) Double labeling with peripherin (green) and TUJ1 (red) in the P1 SGNs and the merged image + DAPI; type II SGNs was negative for peripherin. D,E) Peripherin-positive type II cochlear afferent nerve fibers innervated mainly three rows of OHC. F) Type II SGNs of P5 were immunoreactive for peripherin. G) Peripherin-positive type II cochlear afferent nerve fibers projected beyond the floor of the tunnel of Corti to the OHCs. H,I) Type II SGNs of P8 were immunoreactive for peripherin, peripherin-immunoreactive type II SGNs did not colocalize with TUJ1-labelled SGNs. G,K,L) Double labeling with peripherin (green) and NF200 (red) in the adult SGNs and the merged image + DAPI; peripherin was colocalized with NF200 in the adult SGNs. GER, greater epithelial ridge; IHC, inner hair cell; OHC, outer hair cell; SGN, spiral ganglion neuron.

the cuticular plates of IHCs and OHCs, which further suggest the crucial role of CR in the hearing.⁴⁵ Abnormal expression of CR has been proposed to be associated with the certain disease process, such as Hirschsprung disease and Alzheimer's diseases.^{46,47} Meanwhile, changes in CaBP28K expression have been reported to be involved in hearing impairment caused by thyroid hormone deficiency, which is known to induce numerous functional and morphological deficits in the brain during early developmental stages.⁴⁸ Several studies have reported that thyroid hormone deficiency alters the development of neurons expressing CR in both the central and peripheral nervous systems, and hypothyroidism affects the growth of sensory neurons expressing CR protein mainly during embryonic life.⁴⁹⁻⁵¹ In adult hypothyroid rats, the mean number of CR-positive neurons per spinal cord section was significantly decreased compared to normal adult rats.⁵² It is tempting to speculate that changes in the expression of CR in the SGNs and afferent fibers might also participate in sensorineural hearing loss attributed to hypothyroidism. Our findings of CR immunolocalization suggested a potential link to auditory neuropathy, characterized by normal OHCs function but abnormal neural conduction of the auditory pathway.⁵³

This paper extended and refined previous studies of the spatio-temporal pattern of CR expression in the developing mouse cochlea, demonstrating its specific expression in the developing and adult SGNs, their peripheral neurite processes innervating the IHCs, as well as in sensory hair cells. CR appeared to play a role in the reorganization and establishment of cochlear afferent innervation, which occurs prior to the onset of hearing.

References

- DeFelipe J. Types of neurons, synaptic connections and chemical characteristics of cells immunoreactive for calbindin-D28K, parvalbumin and calretinin in the neocortex. *J Chem Neuroanat* 1997;14:1-19.
- Chen Y, Gu Y, Li Y, Li GL, Chai R, Li W, Li H. Generation of mature and functional hair cells by co-expression of Gfi1, Pou4f3, and Atoh1 in the postnatal mouse cochlea. *Cell Rep* 2021;35:109016.
- Ouji Y, Ishizaka S, Nakamura-Uchiyama F, Wanaka A, Yoshikawa M. Induction of inner ear hair cell-like cells from Math1-transfected mouse ES cells. *Cell Death Dis* 2013;4:e700.
- Huerta JJ, Nori S, Llamas MM, Vázquez MT, Bronzetti E, Vega JA. Calretinin immunoreactivity in human sympathetic ganglia. *Anat Embryol (Berl)* 1996;194:373-8.
- Ordóñez NG. Value of calretinin immunostaining in diagnostic pathology: a review and update. *Appl Immunohistochem Mol Morphol* 2014;22:401-15.
- Dogliani C, Dei Tos AP, Laurino L, Iuzzolino P, Chiarelli C, Celio MR, Viale G. Calretinin: a novel immunocytochemical marker for mesothelioma. *Am J Surg Pathol* 1996;20:1037-46.
- Rogers JH, Résibois A. Calretinin and calbindin-D28k in rat brain: patterns of partial co-localization. *Neuroscience* 1992;51:843-65.
- Liu W, Chen H, Zhu X, Yu H. Expression of Calbindin-D28K in the developing and adult mouse cochlea. *J Histochem Cytochem* 2022;70:583-96.
- Ewert D, Hu N, Du X, Li W, West MB, Choi C, et al. HPN-07, a free radical spin trapping agent, protects against functional, cellular and electrophysiological changes in the cochlea induced by acute acoustic trauma. *PLoS One* 2017;12:e0183089.
- Foran L, Blackburn K, Kulesza RJ. Auditory hindbrain atrophy and anomalous calcium binding protein expression after neonatal exposure to monosodium glutamate. *Neuroscience* 2017;344:406-17.
- Alvarado JC, Fuentes-Santamaría V, Gabaldón-Ull MC, Jareño-Flores T, Miller JM, Juiz JM. Noise-induced "toughening" effect in wistar rats: enhanced auditory brainstem responses are related to calretinin and nitric oxide synthase upregulation. *Front Neuroanat* 2016;10:19.
- Wang M, Lin S, Xie R. Apical-basal distribution of different subtypes of spiral ganglion neurons in the cochlea and the changes during aging. *PLoS One* 2023;18:e0292676.
- Wang M, Zhang C, Lin S, Wang Y, Seicol BJ, Ariss RW, Xie R. Biased auditory nerve central synaptopathy is associated with age-related hearing loss. *J Physiol* 2021;599:1833-54.
- Pangršič T, Gabrielaitis M, Michanski S, Schwaller B, Wolf F, Strenzke N, Moser T. EF-hand protein Ca²⁺ buffers regulate Ca²⁺ influx and exocytosis in sensory hair cells. *Proc Natl Acad Sci USA* 2015;112:E1028-37.
- Imamura S, Adams JC. Immunolocalization of peptide 19 and other calcium-binding proteins in the guinea pig cochlea. *Anat Embryol (Berl)* 1996;194:407-18.
- Pibiri V, Gerosa C, Vinci L, Faa G, Ambu R. Immunoreactivity pattern of calretinin in the developing human cerebellar cortex. *Acta Histochem* 2017;119:228-34.
- Coppens AG, Résibois A, Poncelet L. Immunolocalization of calbindin D28k and calretinin in the dog cochlea during postnatal development. *Hear Res* 2000;145:101-10.
- Dechesne CJ, Rabejac D, Desmadryl G. Development of calretinin immunoreactivity in the mouse inner ear. *J Comp Neurol* 1994;346:517-29.
- Kaiser M, Lüdtke TH, Deuper L, Rudat C, Christoffels VM, Kispert A, Trowe MO. TBX2 specifies and maintains inner hair and supporting cell fate in the organ of Corti. *Nat Commun* 2022;13:7628.
- Dechesne CJ, Winsky L, Kim HN, Goping G, Vu TD, Wenthold RJ, Jacobowitz DM. Identification and ultrastructural localization of a calretinin-like calcium-binding protein (protein 10) in the guinea pig and rat inner ear. *Brain Res* 1991;560:139-48.
- Pack AK, Slepecky NB. Cytoskeletal and calcium-binding proteins in the mammalian organ of Corti: cell type-specific proteins displaying longitudinal and radial gradients. *Hear Res* 1995;91:119-35.
- Sanders TR, Kelley MW. Specification of neuronal subtypes in the spiral ganglion begins prior to birth in the mouse. *Proc Natl Acad Sci USA* 2022;119:e2203935119.
- Hafidi A, Després G, Romand R. Ontogenesis of type II spiral ganglion neurons during development: peripherin immunohistochemistry. *Int J Dev Neurosci* 1993;11:507-12.
- Barclay M, Julien JP, Ryan AF, Housley GD. Type III intermediate filament peripherin inhibits neuritegenesis in type II spiral ganglion neurons in vitro. *Neurosci Lett* 2010;478:51-5.
- Liu WJ, Ming SS, Zhao XB, Zhu X, Gong YX. Developmental expression of high-mobility group box 1 (HMGB1) in the mouse cochlea. *Eur J Histochem* 2023;67:3704.
- Shrestha BR, Chia C, Wu L, Kujawa SG, Liberman MC, Goodrich LV. Sensory neuron diversity in the inner ear is shaped by activity. *Cell* 2018;174:1229-1246.e17.
- Spatz WB, Löhle E. Calcium-binding proteins in the spiral ganglion of the monkey, *Callithrix jacchus*. *Hear Res* 1995;86:89-99.
- He S, Yang J. Maturation of neurotransmission in the developing rat cochlea: immunohistochemical evidence from differential expression of synaptophysin and synaptobrevin 2. *Eur J Histochem* 2011;55:e2.

29. Drescher MJ, Drescher DG, Khan KM, Hatfield JS, Ramakrishnan NA, Abu-Hamdan MD, Lemonnier LA. Pituitary adenylyl cyclase-activating polypeptide (PACAP) and its receptor (PAC1-R) are positioned to modulate afferent signaling in the cochlea. *Neuroscience* 2006;142:139-64.
30. Jovanovic S, Milenkovic I. Purinergic modulation of activity in the developing auditory pathway. *Neurosci Bull* 2020;36:1285-98.
31. Bazwinsky-Wutschke I, Dehghani F. Impact of cochlear ablation on calretinin and synaptophysin in the gerbil anteroventral cochlear nucleus before the hearing onset. *J Chem Neuroanat* 2020;104:101746.
32. Benítez-Temiño B, Hernández RG, de la Cruz RR, Pastor AM. BDNF Influence on adult terminal axon sprouting after partial deafferentation. *Int J Mol Sci* 2023;24:10660.
33. Rogers JH. Two calcium-binding proteins mark many chick sensory neurons. *Neuroscience* 1989;31:697-709.
34. Bastianelli E, Pochet R. Calmodulin, calbindin-D28k, calretinin and neurocalcin in rat olfactory bulb during postnatal development. *Brain Res Dev Brain Res* 1995;87:224-7.
35. Liu WJ, Yang J. Preferentially regulated expression of connexin 43 in the developing spiral ganglion neurons and afferent terminals in post-natal rat cochlea. *Eur J Histochem* 2015;59:2464.
36. Rubel EW, Fritzsche B. Auditory system development: primary auditory neurons and their targets. *Annu Rev Neurosci* 2002;25:51-101.
37. Kang KW, Pangeni R, Park J, Lee J, Yi E. Selective loss of calretinin-poor cochlear afferent nerve fibers in streptozotocin-induced hyperglycemic mice. *J Nanosci Nanotechnol* 2020;20:5515-9.
38. Idrizbegovic E, Salman H, Niu X, Canlon B. Presbycusis and calcium-binding protein immunoreactivity in the cochlear nucleus of BALB/c mice. *Hear Res* 2006;216-217:198-206.
39. Idrizbegovic E, Viberg A, Bogdanovic N, Canlon B. Peripheral cell loss related to calcium binding protein immunocytochemistry in the dorsal cochlear nucleus in CBA/CaJ mice during aging. *Audiol Neurootol* 2001;6:132-9.
40. Jankovski A, Garcia C, Soriano E, Sotelo C. Proliferation, migration and differentiation of neuronal progenitor cells in the adult mouse subventricular zone surgically separated from its olfactory bulb. *Eur J Neurosci* 1998;10:3853-68.
41. von Bohlen Und Halbach O. Immunohistological markers for staging neurogenesis in adult hippocampus. *Cell Tissue Res* 2007;329:409-20.
42. Gonzalez ABI, Koning HK, Tuz-Sasik MU, Osselen IV, Manuel R, Boije H. Perturbed development of calb2b expressing dl6 interneurons and motor neurons underlies locomotor defects observed in calretinin knock-down zebrafish larvae. *Dev Biol* 2024;508:77-87.
43. Chen P, Segil N. p27(Kip1) links cell proliferation to morphogenesis in the developing organ of Corti. *Development* 1999;126:1581-90.
44. Hackney CM, Mahendrasingam S, Penn A, Fettiplace R. The concentrations of calcium buffering proteins in mammalian cochlear hair cells. *J Neurosci* 2005;25:7867-75.
45. Zheng JL, Gao WQ. Analysis of rat vestibular hair cell development and regeneration using calretinin as an early marker. *J Neurosci* 1997;17:8270-82.
46. Singh SK, Gupta UK, Aggarwal R, Rahman RA, Gupta NK, Verma V. Diagnostic role of calretinin in suspicious cases of Hirschsprung's disease. *Cureus* 2021;13:e13373.
47. Brion JP, Résibois A. A subset of calretinin-positive neurons are abnormal in Alzheimer's disease. *Acta Neuropathol* 1994;88:33-43.
48. Diez D, Morte B, Bernal J. Single-cell transcriptome profiling of thyroid hormone effectors in the human fetal neocortex: expression of *SLCO1C1*, *DIO2*, and *THRB* in specific cell types. *Thyroid* 2021;31:1577-88.
49. Nam SM, Kim YN, Yoo DY, Yi SS, Kim W, Hwang IK, et al. Hypothyroid states mitigate the diabetes-induced reduction of calbindin D-28k, calretinin, and parvalbumin immunoreactivity in type 2 diabetic rats. *Neurochem Res* 2012;37:253-60.
50. Shiraki A, Akane H, Ohishi T, Wang L, Morita R, Suzuki K, et al. Similar distribution changes of GABAergic interneuron subpopulations in contrast to the different impact on neurogenesis between developmental and adult-stage hypothyroidism in the hippocampal dentate gyrus in rats. *Arch Toxicol* 2012;86:1559-69.
51. Wallis K, Sjögren M, Hogerlinden MV, Silberberg G, Fisahn A, Nordström K, et al. Locomotor deficiencies and aberrant development of subtype-specific GABAergic interneurons caused by an unliganded thyroid hormone receptor alpha1. *J Neurosci* 2008;28:1904-15.
52. Barakat-Walter I, Kraftsik R, Kuntzer T, Bogousslavsky J, Magistretti P. Differential effect of thyroid hormone deficiency on the growth of calretinin-expressing neurons in rat spinal cord and dorsal root ganglia. *J Comp Neurol* 2000;426:519-33.

Received: 4 September 2024. Accepted: 22 October 2024.

This work is licensed under a Creative Commons Attribution-NonCommercial 4.0 International License (CC BY-NC 4.0).

©Copyright: the Author(s), 2024

Licensee PAGEPress, Italy

European Journal of Histochemistry 2024; 68:4137

doi:10.4081/ejh.2024.4137

Publisher's note: all claims expressed in this article are solely those of the authors and do not necessarily represent those of their affiliated organizations, or those of the publisher, the editors and the reviewers. Any product that may be evaluated in this article or claim that may be made by its manufacturer is not guaranteed or endorsed by the publisher.